FIRST OPERATION OF A 432-MHz, 3-MeV RFQ STABILIZED WITH PISLs

Akira Ueno, Yoshishige Yamazaki, *Satoshi Fujimura, Chikashi Kubota, Kazuo Yoshino, Yuuichi Morozumi, Masato Kawamura, Kikuo Kudo, Masaaki Ono, Shozo Anami, Zenei Igarashi, Eiichi Takasaki, Akira Takagi, Yoshiharu Mori and Motohiro Kihara
National Laboratory for High Energy Physics, KEK
**Graduate University for Advanced Studies*
1-1 Oho, Tsukuba-shi, Ibaraki-ken, 305, Japan

Abstract

A 432-MHz, 3-MeV radio-frequency quadrupole (RFQ) linac was developed as a pre-injector of the 1-GeV proton linac for the Japanese Hadron Project (JHP). This four-vane-type RFQ was stabilized against dipole mode mixing with newly devised -mode stabilizing loops (PISLs). In this paper, the results of the first beam test of the RFQ are presented. The RFQ accelerated a 6.5 mA proton beam, which was injected from a multicusp proton ion source.

Introduction

A radio-frequency quadrupole (RFQ) linac has been developed as a pre-injector of the 1-GeV proton linac for the Japanese Hadron Project (JHP) [1]. Its resonant frequency, duty factor, peak beam current, injection and final energies were determined from a beam-optics consideration of the entire system to be 432 MHz, 3% (600 μsx50 Hz), 20 mA, 50 keV and 3 MeV, respectively. In order to determine the cell parameters of the RFQ we first studied two typical beam-dynamics design codes for RFQs. One was the RFQUIK developed for high-current proton RFQs [2]; the other was the GENRFQ developed for low-current heavy-ion RFQs [3]. However, the design with the RFQUIK resulted in a large longitudinal emittance and a long cavity length, while the design with the GENRFQ resulted in a small current limit. We therefore developed a new design procedure in order to optimize the beam-dynamics design of intermediate- or high-beam current RFQs, such as that for the JHP. This design procedure was programmed in the computer code package KEKRFQ [4]. When we designed the JHP RFQ with these three codes, the cavity length of the design with the KEKRFQ or the GENRFQ was about 80% of that with the RFQUIK. Here, the longitudinal emittance and the current limit were estimated by simulating the beam dynamics with the computer code PARMTEQ [5]. The simulated longitudinal emittance of the design with the KEKRFQ was about 60% of that with the RFQUIK and about 90% of that with the GENRFQ. The simulated current limit of the design with the KEKRFQ was also improved by more than 10% compared with that with the GENRFQ. Therefore, we used the cell parameters optimized with the KEKRFQ for the JHP RFQ.

In order to precisely compare measurements of the accelerated beam with the simulation results, the focusing and accelerating electric field in the RFQ should be as uniform as possible. However, the frequency separations between the accelerating mode (TE_{210} mode) and the several dipole modes (TE_{11n} mode) are significantly small in a long four-vane type RFQ without any field stabilizer. These dipole modes therefore easily mixed with the accelerating mode due to a small amount of perturbation. In order to practically avoid any dipole mode mixing, several pairs of vane coupling rings (VCRs) [6] have been frequently used so far. However, the VCR has a complicated shape and is difficult to fabricate. In particular, cooling the VCR and the electrical contact between the VCR and the vanes (important for the high duty operation) are very difficult. We therefore devised a -mode stabilizing loop (PISL) as a new field-stabilization method for high-duty, four-vane-type RFQs [7,8]. By installing several pairs of PISLs to the JHP RFQ, we obtained a uniform field distribution within ±0.75% both azimuthally and longitudinally [9]. It is noted that the longitudinal electric-field distortion due to the PISL (1.5%) is much smaller than that due to the VCR (5%). The validity of the new design procedure will be confirmed empirically during beam acceleration with the fairly uniform and stable electric field of the JHP RFQ. After 170 hours of high-power operation, the RFQ was successfully conditioned up to the design rf power level of 500 kW with a 1.5% duty factor (315 μsx50 Hz, a half of the design value) [10].

In this paper, we present the results of the first beam test of the JHP RFQ.

Experimental Set-up

First, the experimental set-up is described in drawings. A schematic drawing of the multi-cusp proton ion source is shown in Fig. 1. The beam extracted from the ion source was focused into the

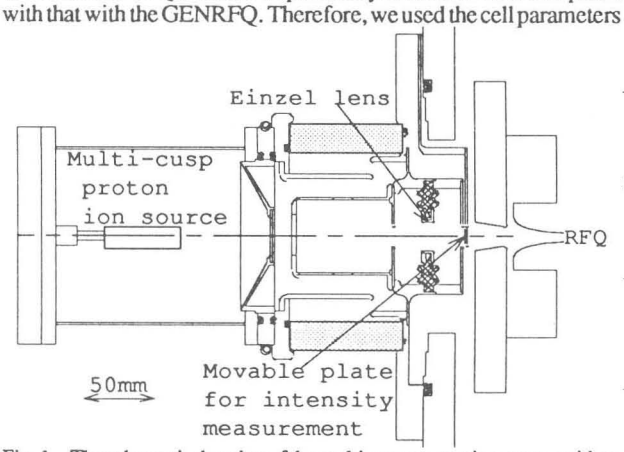

Fig. 1 The schematic drawing of the multi-cusp proton ion source with an einzel lens.

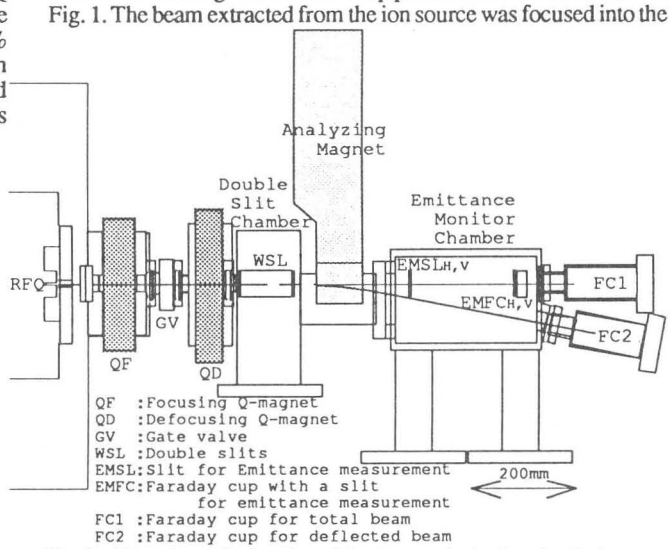

Fig. 2 The schematic drawing of the diagnostic devices for the beam ejected from the RFQ.

RFQ by an einzel lens located at the beam entrance of the RFQ. The beam intensity injected to the RFQ was measured by inserting a movable aluminum plate on the beam axis, which was located in between the einzel lens and the RFQ. In order to suppress secondary electrons from the plate, the plate was biased to +90 V by connecting the plate with the positive electrode of a 90-V battery, the negative electrode of which was connected to ground. The beam intensity was calculated based on the measured voltage induced in a 500- resistance, which was located between the plate and the 90-V battery.

Diagnostic devices for a beam ejected from the RFQ are schematically shown in Fig. 2. With these devices, we measured: (1) the total beam intensity, (2) the intensity of the accelerated beam, (3) the energy and energy spread, (4) the horizontal emittance and (5) the vertical emittance, as follows:

(1) The total beam intensity was measured with Faraday cup FC1. FC1 was connected to ground through a 50- resistance. The beam intensity was calculated based on the voltage induced in the resistance.

(2) The beam ejected from the RFQ was analyzed by an analyzing magnet (a coil current of 57.5 A and a bending strength of BL=0.0483 T·m). The component of the beam deflected by around 11 °, the energy of which was estimated to be about 3 MeV, was detected with Faraday cup FC2. The output current from FC2 was terminated with a 50- resistance in the same way as FC1.

(3) The beam ejected from the RFQ was cut by inserted movable double slits (WSL) on the beam axis. The distance between the two slits of WSL was 100 mm. Each slit was made of two aluminum plates with a thickness of 1 mm and a gap between the two plates of 0.4 mm. The thus-narrowed beam was analyzed by the analyzing magnet and detected with the movable Faraday cup $EMFC_H$ with a slit for the horizontal emittance measurement. The same type of slit as that used for WSL was attached to $EMFC_H$. The distance by which $EMFC_H$ was removed from the standard position was inversely proportional to the momentum of the detected beam. Therefore, the energy and energy spread of the accelerated beam could be calculated based on the dependence of the beam current on the position of $EMFC_H$. In this paper, the energy of the accelerated beam stands for the value calculated from $EMFC_H$ position where the largest beam intensity was detected.

(4) By moving the movable slit ($EMSL_H$) for the horizontal emittance measurement step by step from one end of the beam to the other end, each portion of the beam was cut out through the slit of $EMSL_H$. The slit was of the same type as that used for WSL. Each portion of the beam was detected with $EMFC_H$. At that time, $EMFC_H$ was also moved step by step. We could thus map the horizontal emittance in x-x' phase space, since the divergence of the beam could be calculated from the relative position between $EMSL_H$ and $EMFC_H$. (The distance between $EMSL_H$ and $EMFC_H$ was 205 mm.)

(5) The vertical emittance was measured in the same way as the horizontal emittance. This time, we used the movable slit $EMSL_V$ and the movable Faraday cup $EMFC_V$ with a slit.

Results of the First Beam Test

The beam intensity injected into the RFQ was detected by inserting a movable plate on the beam axis (described in the previous section). The measured signal is shown in Fig. 3. Here, the measured intensity is 40 mA. We carried out a mass analysis of the ejected beam from the RFQ when no rf power was fed into the RFQ. The analyzing magnet and $EMFC_H$ were used as a mass analyzer. Since the measured proton ratio of the beam was 70%, the injected proton intensity was estimated to be 28 mA.

The ejected beam from the RFQ, when a peak rf power of 480 kW was fed into the RFQ, was analyzed with the analyzing magnet and detected with FC2. The measured beam signal is shown as the top trace of Fig. 4. The bottom trace of Fig. 4 shows the rf level in the RFQ. A coil current of 57.5 A for the analyzing magnet deflected the accelerated 3-MeV proton beam to FC2. The measured peak beam intensity was 6.5 mA, where the voltage loaded on the einzel lens was 45 kV. The fluctuation of the focusing strength of the einzel lens due to the beam loading seems to cause a variation in the beam intensity within the pulse duration. We must modify the beam-transport line between the ion source and the RFQ in order to improve the emittance matching.

We measured the energy of the accelerated beam with WSL, the analyzing magnet and $EMFC_H$. The energy estimated from the position of $EMFC_H$ (3.2 MeV) was significantly higher than the simulated value (3.01MeV). Since the distance between WSL and the analyzing magnet was very close, the fringing field was not negligible. The beam was probably bent in WSL by the fringing field of the analyzing magnet. In order to take into account the effect of the fringing field, the dependences of the $EMFC_H$ position, where either the accelerated proton beam or the 50 keV H_3^+ beam was detected, on the coil current of the analyzing magnet were measured as shown in Fig. 5. From the slopes of these two dependences, the energy of the accelerated beam was calculated to be 3.06MeV. This value is also slightly higher than the simulated value. The measurement error of the coil current of the analyzing magnet is one of possible reasons for this slight discrepancy.

The energy spread of the accelerated beam was measured with WSL, the analyzing magnet and $EMFC_H$, where the coil current of the analyzing magnet was 57.5 A. The results for three different vane voltages normalized with the design value (0.9, 1.0 and 1.1) are shown in Fig. 6. The beam measured at a normalized vane voltage of 0.9 is accompanied by a low-energy tail. The measured energy spread (about 200 keV) at the design vane voltage was 2.5-times as large as the simulated value of 80 keV. The energy

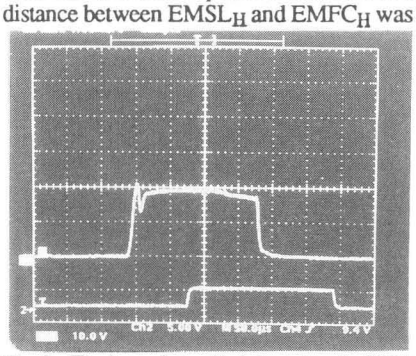

Fig. 3 The beam intensity injected to the RFQ (the top trace) and the rf level in the RFQ (the bottom trace).

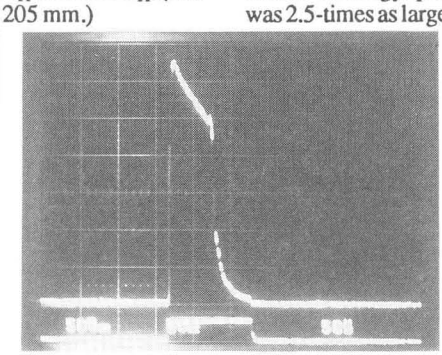

Fig. 4 The accelerated proton beam intensity detected with the FC2 (the top trace) and the rf level in the RFQ (the bottom trace).

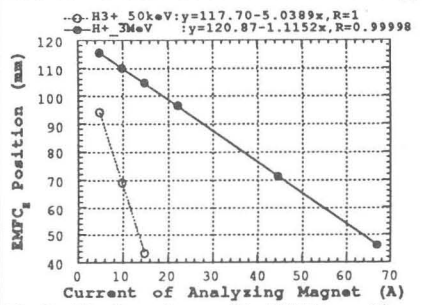

Fig. 5 The dependences of the $EMFC_H$ positions, where the accelerated proton beam and the 50 keV H_3^+ beam were detected, on the coil current of the analyzing magnet.

resolution was probably degraded by the too large gaps (0.4 mm) of the slits for WSL and $EMFC_H$. It is noted that the energy spread at a normalized vane voltage of 1.1 was smaller than that at the design vane voltage.

We measured the dependence of the accelerated beam intensity on the normalized vane voltage (Fig. 7). Although the transmission of the beam is relatively low at a normalized vane voltage of 1.1, the energy spread is small, as described in the previous paragraph. It could be interesting to see if these results can be reproduced by a simulation.

The horizontal and vertical emittances were measured with $EMSL_{H,V}$ and $EMFC_{H,V}$. The measured emittances in real phase space are shown in Figs. 8a (horizontal emittance) and 8b (vertical emittance). In these figures, each emittance is shown by nine contours. Each contour stands for 90, 80, , , or 10% emittance. The simulated emittances are shown by the solid line ellipses. The relationships between the normalized emittances and the beam fractions are shown in Figs. 9a (horizontal emittance) and 9b (vertical emittance). The measured 90% emittances (about 2.4 mm•mrad) are significantly larger than the simulated value (1.1 mm•mrad). Too large gaps (0.4 mm) of the slits for $EMSL_{H,V}$ and $EMFC_{H,V}$ probably cause this discrepancy.

Conclusions

The first beam-acceleration test of the RFQ developed for the JHP was performed. When a proton beam of 28 mA was injected into the RFQ, we obtained a 6.5 mA accelerated beam. The emittance of the injected beam was probably mismatched with the acceptance of the RFQ. The measured beam energy of 3.06 MeV is slightly higher than the simulated value of 3.01 MeV. The measurement error of the analyzing magnet current is one of the possible reasons for this difference. The measured 90% normalized emittance of 2.4 mm•mrad was significantly larger than the simulated value of 1.1 mm•mrad. Too large gaps (0.4 mm) of the slits used in the emittance monitors probably gave rise to this discrepancy.

We plan to improve the beam-transport line between the ion source and the RFQ in order to obtain the design beam intensity of 20 mA. We are also going to improve the resolution of the energy analyzer and the emittance monitors in order to more meaningfully compare the measurements with the simulation results.

Acknowledgement

The authors wish to express their sincere thanks to Kazuyuki Suzuki and the other members of the Nuclear Equipment Design Section and the Tools Section at Hitachi Works, Hitachi, Ltd. for their technical support.

References

[1] Y. Yamazaki and M. Kihara, Proc. 1990 Lin. Accel. Conf., **LA-12004-C**, 543, (1991).
[2] K. R. Crandall et al., IEEE Trans. Nucl. Sci., **Vol. NS-26**, 3469 (1979).
[3] T. Nakanishi et al., Part. Accel., **20**, 183 (1987).
[4] A. Ueno and Y. Yamazaki, Proc. 1990 Lin. Accel. Conf., **LA-12004-C**, 329, (1991).
[5] K. R. Crandall and T. P. Wangler, AIP Conf. Proc. 177, 22 (1988).
[6] H. R. Schneider and H. Lancaster, IEEE Trans. Nucl. Sci., **NS-30**, (4),3007, (1983).
[7] A. Ueno and Y. Yamazaki, Nucl. Instr. and Meth. **A300**, 15, (1991).
[8] A. Ueno, T. Kato and Y. Yamazaki, Proc. 1990 Lin. Accel. Conf., LANL report, **LA-12004-C**, 57, (1991).
[9] A. Ueno and Y. Yamazaki, "Low-power RF Characteristics of a 432-MHz, 3-MeV RFQ Stabilized with PISLs", in this conference.
[10] A. Ueno et al., "High-power Test of a 432-MHz, 3-MeV RFQ Stabilized with PISLs", in this conference.

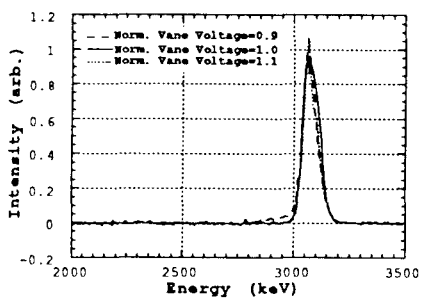

Fig. 6 The measured energy spreads when the coil current of the analyzing magnet were 57.5 A.

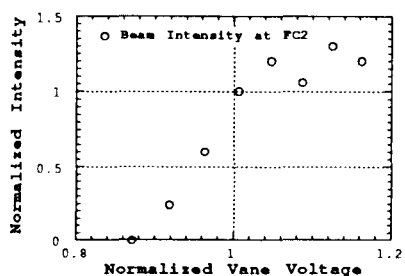

Fig. 7 The measured dependence of the accelerated proton beam intensity on the normalized vane voltage.

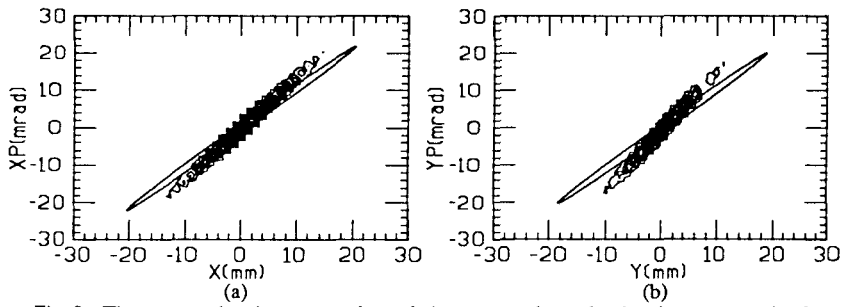

Fig. 8 The measured emittances on the real phase space shown by the nine contours (each contour stands for 90, 80, , , or 10% emittance) and the simulated emittances shown by the solid line ellipses : (a) horizontal emittance and (b) vertical emittance.

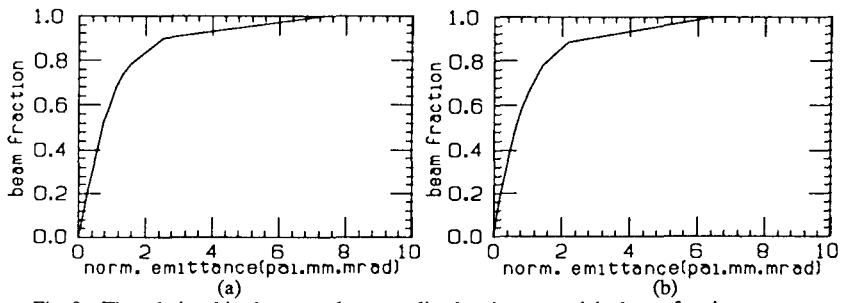

Fig. 9 The relationships between the normalized emittance and the beam fraction : (a) horizontal emittance and (b) vertical emittance.